INVENTORY OF SUPPLEMENTARY MATERIAL

Supplemental material includes following items:

- 12 Supplementary Figures
- 2 Supplementary Tables

- **Supplementary Figure S1** Comparison of FcεRI expression and surface IgE loading in IgE_R-TG and WT animals.
- **Supplementary Figure S2** Characterization of background- and age-related effects on IgE and IgG1 levels in IgE_R-TG mice.
- **Supplementary Figure S3** Flow cytometric analysis of CD23 expression on splenocytes of IgE_R-TG and WT animals.
- **Supplementary Figure S4** Characterization of IgE/FcεRI-derived signals in DCs (microarray analysis)
- **Supplementary Figure S5** Further characterization of the food allergy model.
- **Supplementary Figure S6** Additional parameters determined in the asthma model.
- **Supplementary Figure S7** House dust mite (HDM)-induced airway inflammation in WT and IgE_R-TG animals.
- **Supplementary Figure S8** Additional characterization of the T cell phenotype induced via IgE/FcεRI-mediated antigen presentation.
- **Supplementary Figure S9** Additional data regarding antigen-mediated IgE/FcεRI cross-linking.
- **Supplementary Figure S10** Characterization of mast cell progenitor cultures and their migratory behavior.
- **Supplementary Figure S11** Antigen-specific IgE/FcεRI-crosslinking on LPS-activated murine or human DCs does not inhibit upregulation of co-stimulatory molecules.
- **Supplementary Figure S12** The immune regulatory function of IgE/FcεRI-mediated DC activation **(**model).

- Table S1: **mRNA expression pattern of bm-DCs**
- Table S2: **mRNA expression pattern of small intestinal tissue from a representative food allergy experiment.**

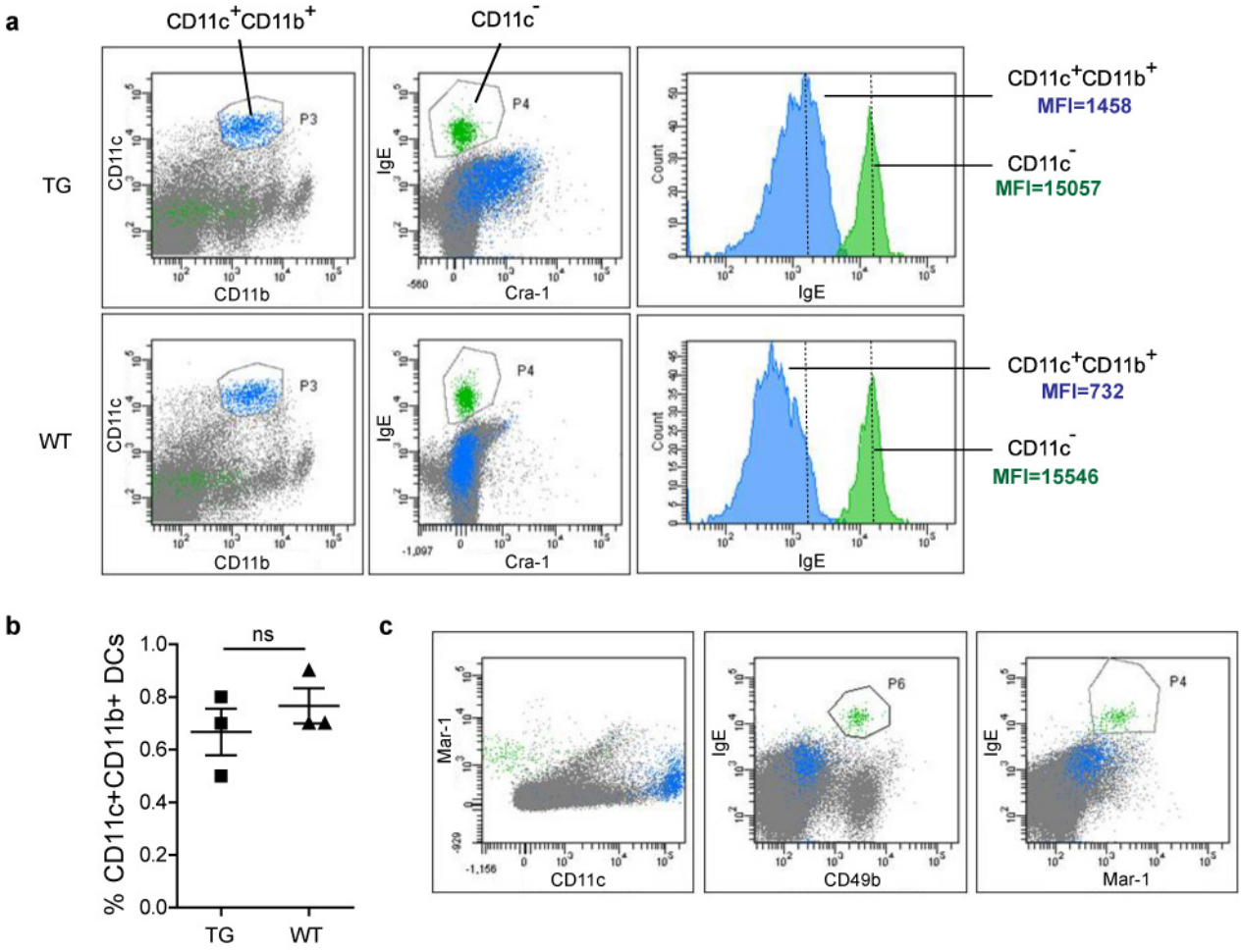

Supplementary Figure S1 Comparison of FcεRI expression and surface IgE loading in IgE_R-TG and WT animals. **(a)** Splenocytes from IgE_R-TG and WT animals were stained for $CD11c^+CD11b^+$ DCs, IgE and human FcεRI expression (Cra-1). In IgE_R-TG animals, $CD11c^+CD11b^+$ DCs express human FcεRI (depicted in blue) and are loaded with low to moderated levels of IgE at steady state. **(b)** IgE_R-TG and WT animals display similar numbers of $CD11c^+CD11b^+$ DCs in the spleens. Percentages are representative of 3 individual mice. **(c)** Gating strategy for basophils. Cells were analyzed for their expression of murine FcεRI (Mar-1) and the basophil marker CD49b. In the spleen, $CD11c^-$ cells with high IgE surface loading (in green) were identified as basophils by their co-expression of CD49b and the murine FcεRI.

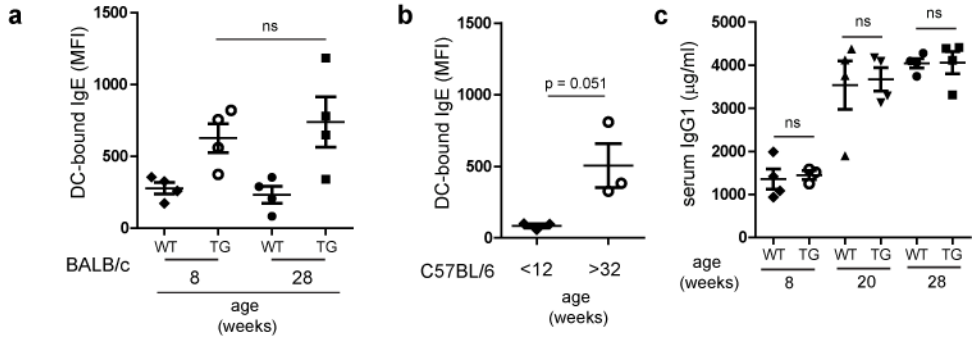

Supplementary Figure S2 Characterization of background- and age-related effects on IgE and IgG1 levels in IgE_R-TG mice. **(a)** No significant increase in the DC-bound IgE pool in mice on the BALB/c background is found between 8 and 28 weeks of age. **(b)** On the C57BL/6 background, the DC-bound IgE in mice increases with age. **(c)** Serum IgG1 levels increase similarly with age in WT and IgER-TG (Balb/c) animals.

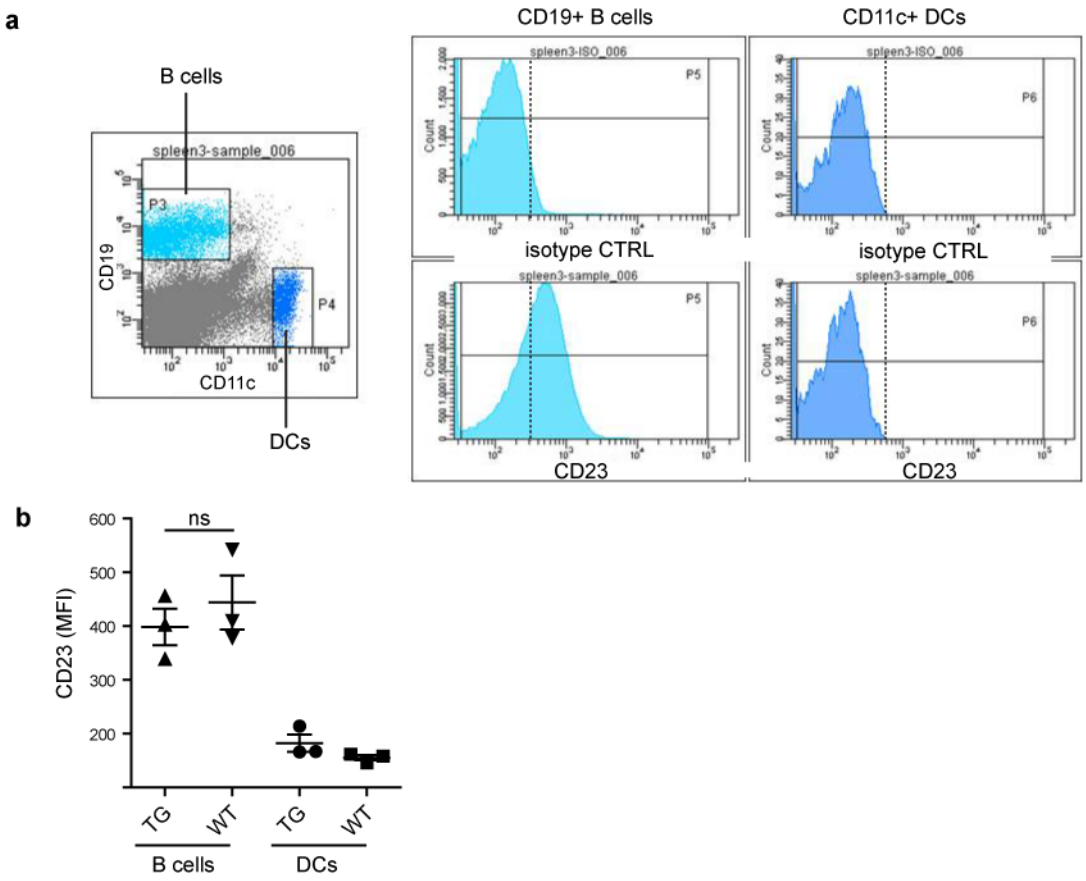

Supplementary Figure S3 Flow cytometric analysis of CD23 expression on splenocytes of IgE_R-TG and WT animals. **(a)** CD23 is expressed on B cells but not on murine DCs. $CD19^+$ B cells and $CD11c^+$ DCs were gated (dot plot) and analyzed for CD23 expression (histograms). **(b)** Mean fluorescence intensity (MFI) of CD23 on B cells and DCs of 3 individual mice is depicted.

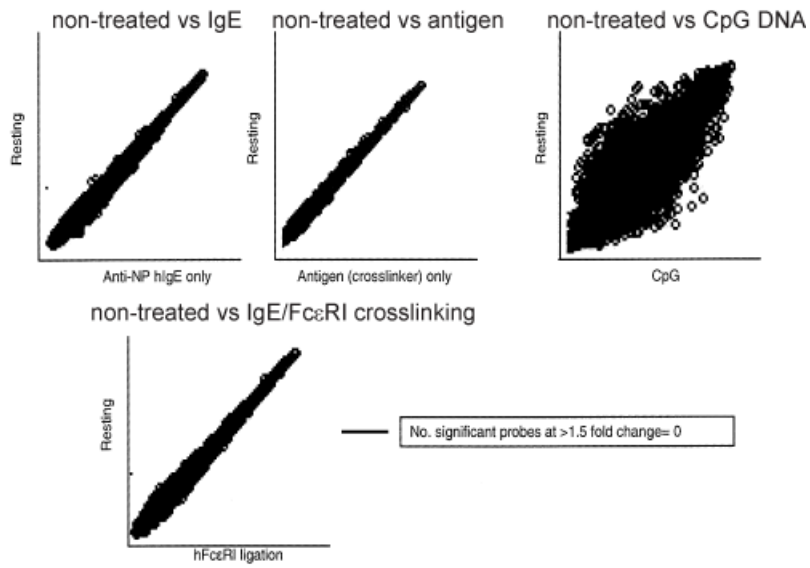

Supplementary Figure S4 Characterization of IgE/FcεRI-derived signals in DCs. Microarray analysis performed with bone marrow-derived cDCs. Data represent the average of 2 experiments performed in triplicates at 24 h and 48 h post stimulation. Unstimulated cells (non-treated) were compared with cells incubated with NP-specific IgE alone, NP-OVA (antigen) alone, CpG DNA, or NP-specific IgE plus NP-OVA (FcεRI crosslinking). Data were analyzed with GenePattern seeking for transcripts regulated by a factor of 1.5 over controls. Of note, DCs used for the microarray analysis were from a different available FcεRI-humanized mouse model (i.e. FcεRIα-TG; Ref. (33)).

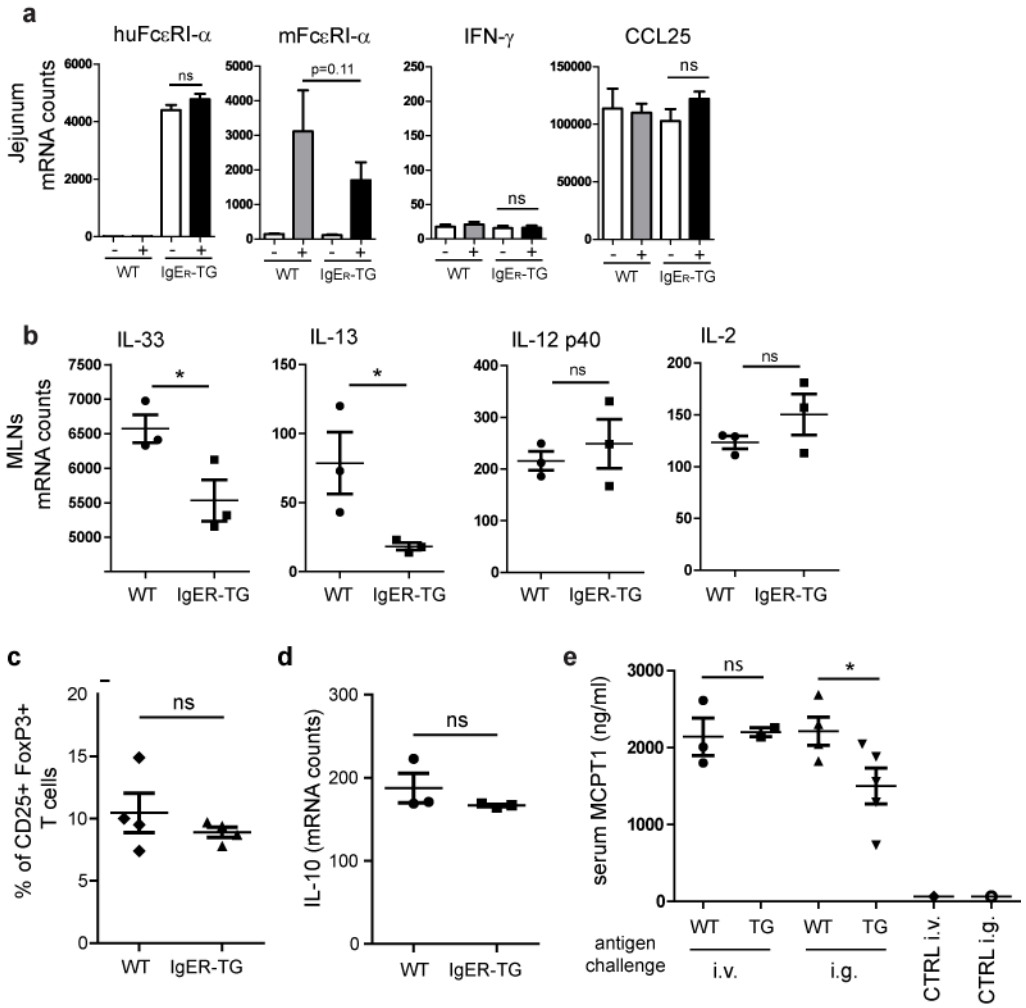

Supplementary Figure S5 Further characterization of the food allergy model. **(a)** Additional data sets of mRNA profiling of GI tissue. Tissue mRNA levels of human and murine FcεRIα-chain (huFcεRIα and mFcεRIα). IFN-γ is expressed at low levels and expression remains unaltered upon sensitization and challenge (+). Transcript levels of CCL25, a chemokine abundantly expressed in the small intestine, did not change. **(b)** mRNA expression levels in the MLNs of food allergic mice. **(c)** Comparative analysis of Tregs and **(d)** IL-10 mRNA expression levels in WT and IgE_R-TG animals **(e)** Mast cell protease 1 (MCPT1) levels in serum are lower in IgE_R-TG mice after intra-gastric (i.g.), but not after intravenous (i.v.) antigen challenge. Control mice received PBS. Serum MCTP1 levels were measured 1 h after antigen challenge.

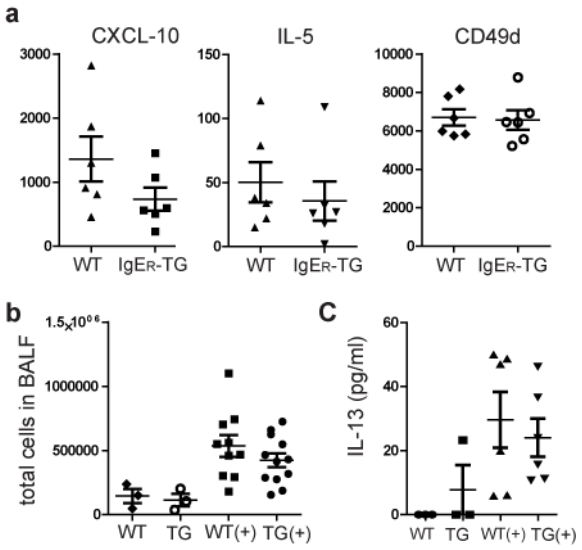

Supplementary Figure S6 Additional parameters determined in the asthma model. (**a**) Additional data sets of mRNA profiling of lung tissue after allergic asthma induction. CD49d (integrin alpha subunit) is shown as one example of unaltered transcript levels. **(b)** Counts of total cells in the bronchoalveolar lavage fluid (BALF) of non-treated mice and sensitized (+) WT and IgE_R-TG mice. **(c)** IL-13 levels in BALF. Symbols represent individual mice of 2 independent experiments.

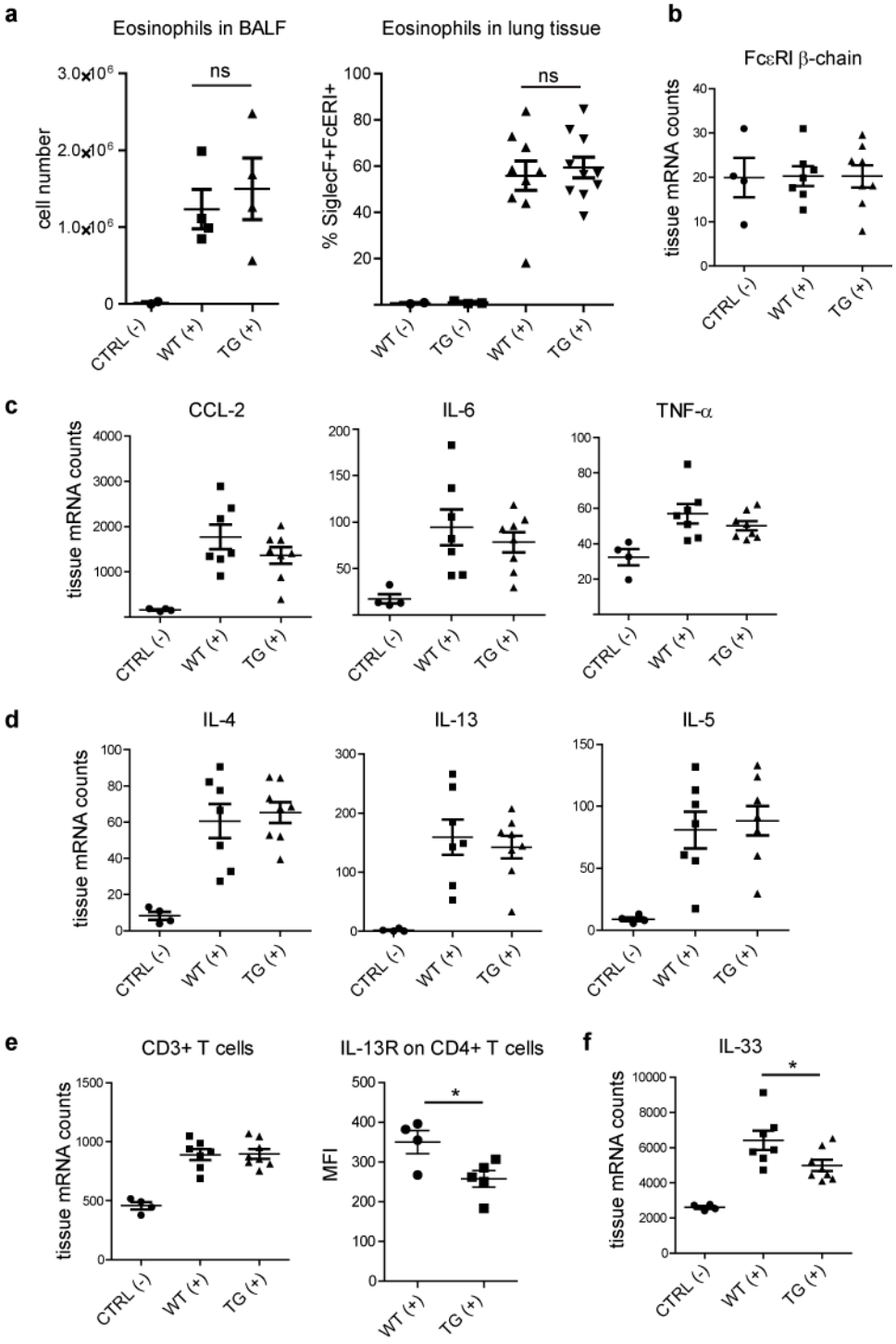

Supplementary Figure S7 House dust mite (HDM)-induced airway inflammation in WT and IgE_R-TG animals. (**a**) Assessment of eosinophil infiltration in BALF and lung tissue. **(b-d)** mRNA profiling of lung tissue. **(e)** $CD4^+$ T cells in the lungs of HDM-sensitized (+) IgE_R-TG animals express lower levels of IL-13 receptor compared to sensitized WT animals. **(f)** IL-33 expression is higher in the lungs of HDM-sensitized WT animals. All symbols represent individual mice of 2 independent experiments.

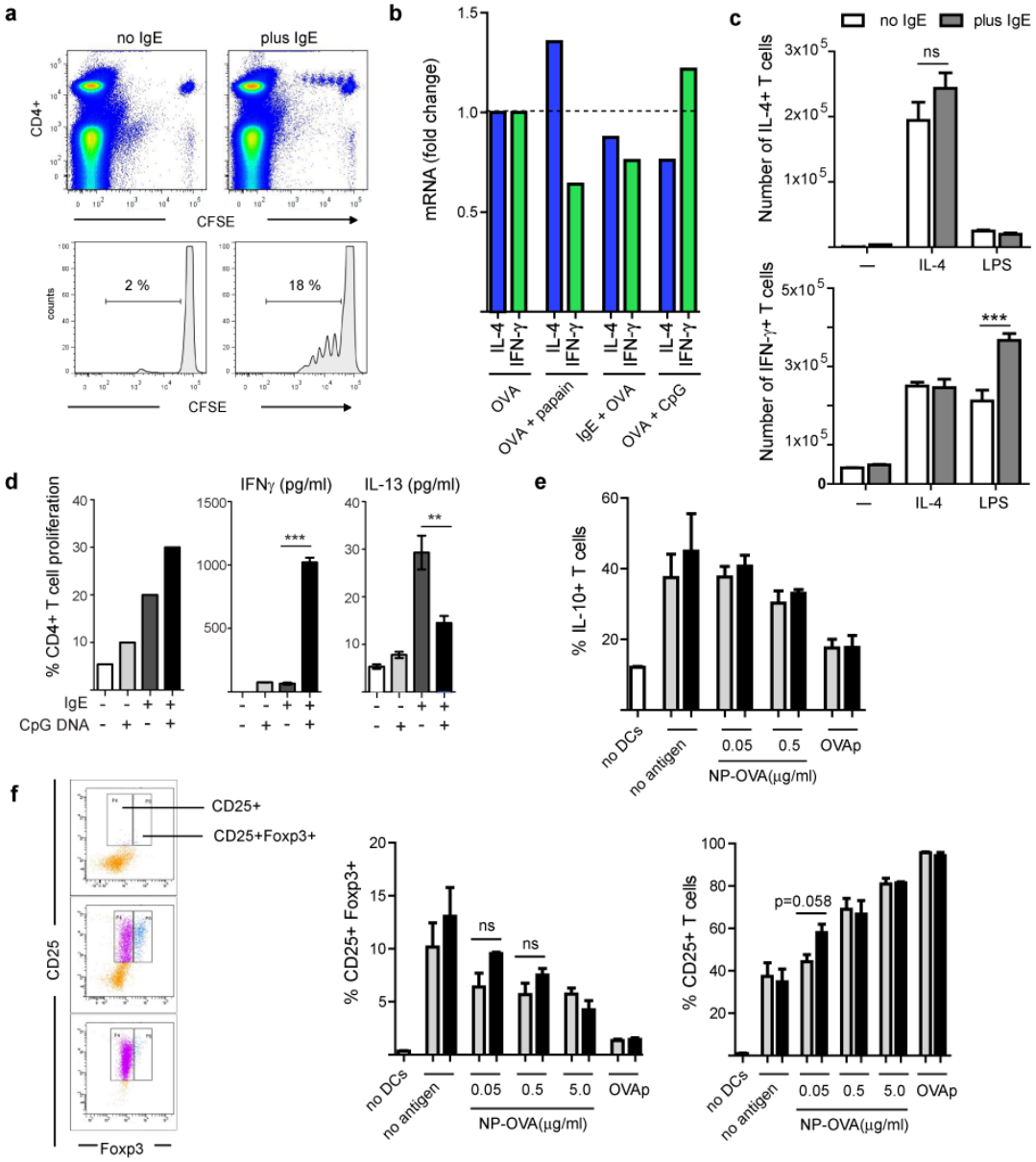

Supplementary Figure S8 Additional characterization of the T cell phenotype induced via IgE/FcεRI-mediated antigen presentation. **(a)** *In vivo* OT-II T cell proliferation assay. Splenic DCs were incubated with IgE-containing (plus) or control (no) medium and loaded with 0.05 μg/ml NP-OVA in vitro before injected into recipient mice. Representative experiment (n=3). **(b)** Papain treatment of DCs induces a Th2 profile *in vivo*, but IgE-mediated antigen uptake does not. DCs were stimulated as indicated. After in vivo proliferation for 3 days, $CD4^+$ T cells from were isolated and IL-4 and IFN-γ expression was determined. **(c)** Corresponding total cell numbers to data presented in Figure 7f. **(d)** *In vitro* antigen presentation assay in the presence of CpG DNA. IFN-γand IL-13 production was measured at day 3 in the DC/T cell co-cultures. **(e)** *In vitro* antigen presentation assay. Priming of IL-10 expressing T cells in the presence of TGF-β1 is not influenced by IgE-mediated antigen uptake. Intracellular cytokine staining day 6 (n=2). **(f)** *In vitro* generation of iTregs is not significantly affected by IgE-mediated antigen uptake by DCs. Naïve $CD4^+CD25^-$ OT-II T cells were co-cultured with DCs and TGF-β1or 6 days. FACS blot show gating strategy for $CD25^+$ $Foxp3^+$ cells (top to bottom: T cells in the absence of DCs, DC stimulated with antigen, and DCs treated with OVAp).

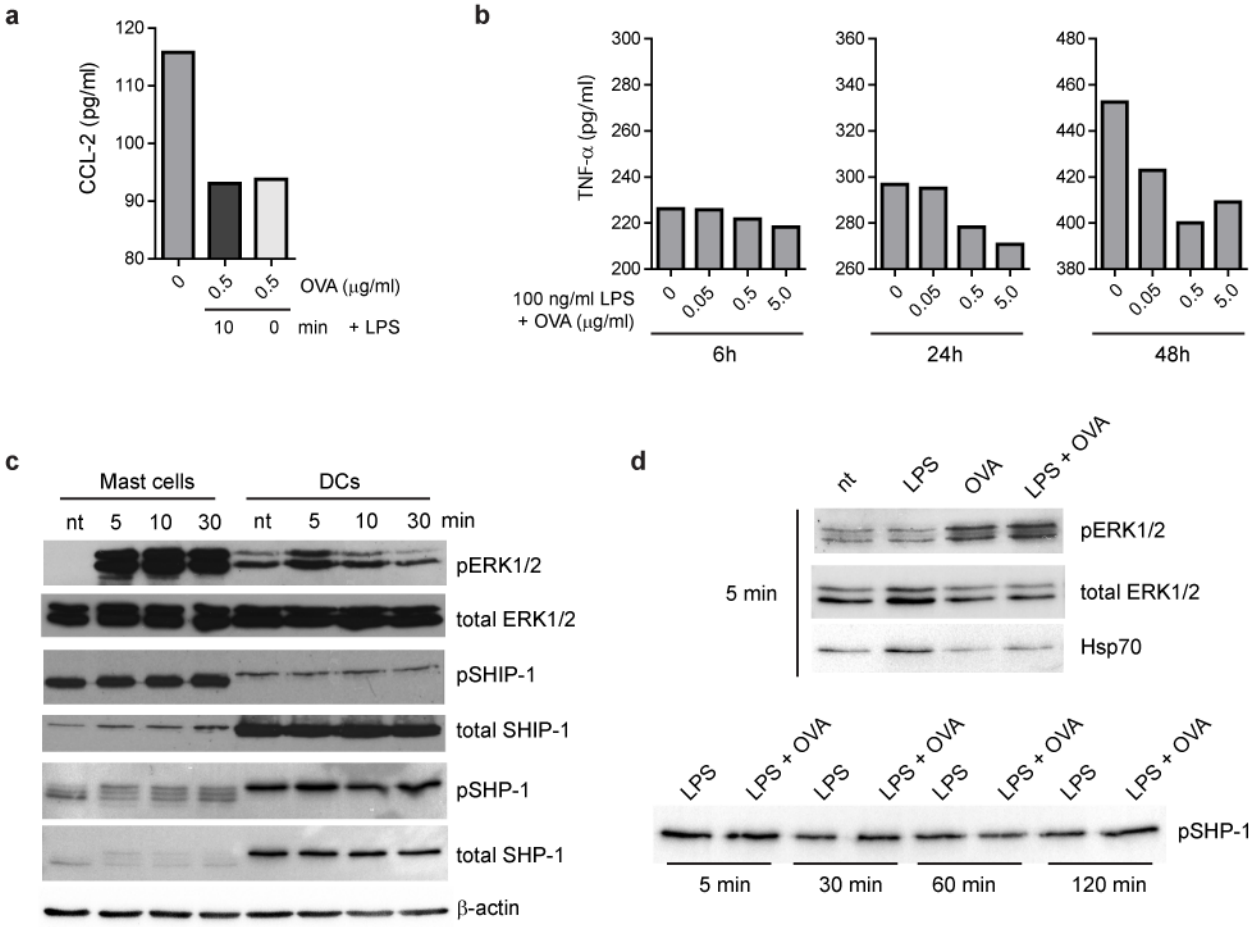

Supplementary Figure S9 Additional data regarding antigen-mediated IgE/FcεRI cross-linking. **(a)** LPS-induced CCL-2 production is inhibited independently of simultaneous or consecutive FcεRI cross-linking. IgE-loaded DCs were stimulated with LPS (all conditions). Indicated concentrations of OVA were added for IgE/ FcεRI crosslinking, either simultanously with LPS (0 min) or after 10 min. Culture supernatant was harvested after 48h and CCL-2 production was analyzed by ELISA. Data are represeative of pooled triplicates. **(b)** Time course and antigen dose response experiments. DCs were stimulated with indicated concentrations of OVA and cell culture supernatants were analyzed after 6h, 24h and 48h. Inhibition of CCL-2 production becomes more obviosue over the time course. **(c)** Comparison of signaling events induced upon antigen-mediated FcεRI cross-linking in mast cells and DCs. Bone-marrow derived mast cells and DCs were pre-loaded with NP-specific IgE. Receptor crosslinking was induced with 0.5µg/ml NP-OVA, cell extracts were prepared after indicated time points, and signaling molecules were analyzed by immunoblot. **(d)** FcεRI cross-linking does not lead to increased SHP-1 phosphorylation upon LPS co-stimulation. IgE-loaded DCs were co-stimulated with LPS and NP-OVA as indicated and signaling molecules were analyzed by immunoblot.

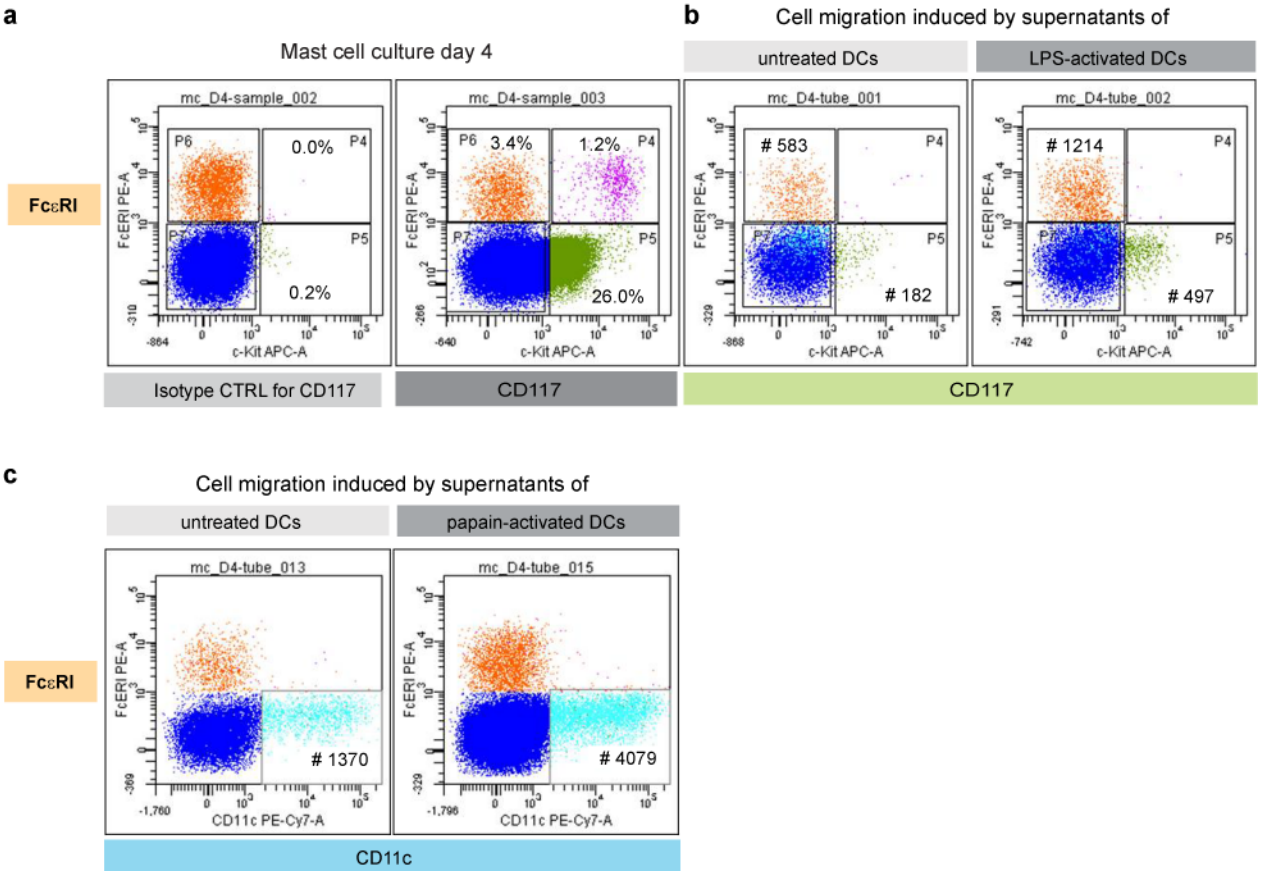

Supplementary Figure S10 Characterization of mast cell progenitor cultures and their migratory behavior. **(a)** Bone marrow cells were cultured with IL-3 and SCF for 4 days and analyzed by FACS (left dot plots). Early mast cell cultures contain cKit$^+$ progenitor cells, few cKit$^+$FcERI$^+$ mast cells, basophils (cKit$^-$ FcERI$^+$) and CD11c$^+$cells (see dot plots in c). **(b)** Supernatants of LPS-activated DCs promote migration of cKit$^+$ mast cell progenitors but not of cKit$^+$FcERI$^+$ mast cells. **(c)** Migration of CD11c$^+$ cells induced by supernatants of papain-activated DCs.

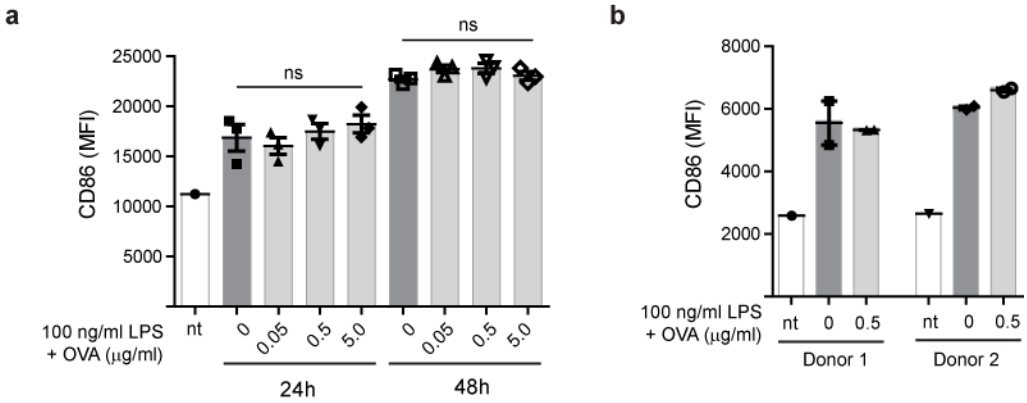

Supplementary Figure S11 Antigen-specific IgE/FcεRI-crosslinking on LPS-activated murine or human DCs does not alter upregulation of co-stimulatory molecules. **(a)** Murine DCs isolated from spleens were pre-loaded with NP-specific IgE before stimulation with indicated concentrations of NP-OVA and LPS for 24h and 48h. Data represent MFI of CD86 from biological triplicates (nt = not treated, n=2). **(b)** Analysis of CD86 expression on human monocyte-derived DCs from 2 different donors. Samples were treated as indicated and analyzed after 24h. Biological duplicates are shown.

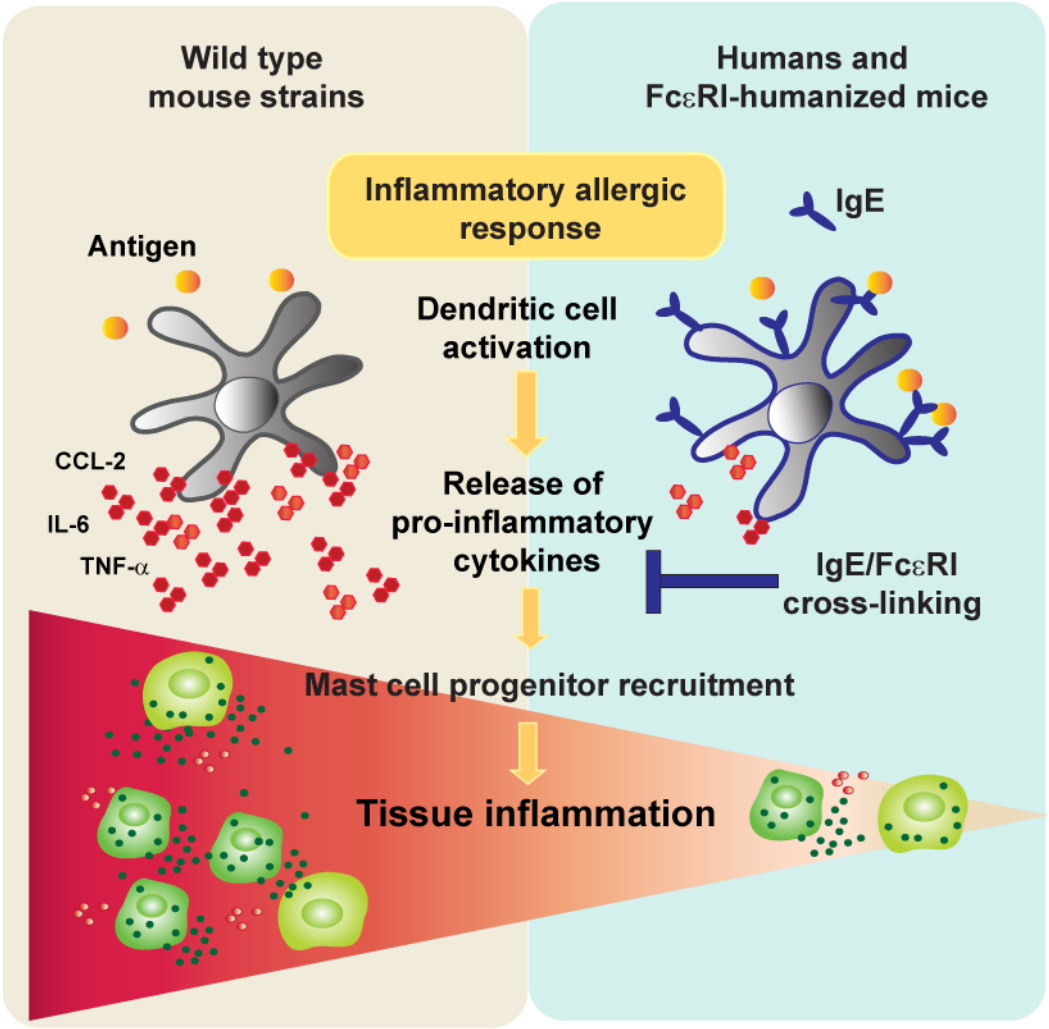

Supplementary Figure S12 The immune regulatory function of IgE/FcεRI-mediated DC activation. DCs produce inflammatory cytokines and chemokines during allergic responses. IgE/FcεRI-mediated DC activation inhibits release of these allergy promoting mediators and thereby restrains mast cell infiltration and allergic tissue inflammation.

Table S1: **mRNA expression pattern of bm-DCs** (* counts < 25 = at detection limit).

	NP-OVA		NP-OVA + IgE		NP-OVA plus CpG DNA		NP-OVA plus papain	
mRNA* (direct counts)	Mean	+/- SEM	Mean	+/- SEM	Mean	+/- SEM	Mean	+/- SEM
arginase1	26	6	28	2	44	7	36	3
CCL1	10	2	9	2	67	13	18	3
CCL11 (eotaxin)	5	1	7	1	10	3	10	3
CCL12 (MCP-5)	9	2	7	0	15	2	35	5
CCL17 (TARC)	20	2	24	5	518	17	251	12
CCL19 (MIP-3β)	11	2	10	5	20	0	16	2
CCL2	11	2	13	1	49	11	88	5
CCL-20 (MIP-3α)	10	0	8	2	12	1	12	3
CCL22 (MDC)	4834	65	5231	133	34260	1517	35968	197
CCL3 (MIP-1α)	113	5	107	16	7864	303	1768	74
CCL4 (MIP-1β)	19	3	20	3	1072	97	150	7
CCL5 (RANTES)	10938	26	12189	414	18512	893	39863	557
CCL7 (MCP-3)	28	4	36	1	46	3	56	4
CCL8 (MCP-2)	14	1	15	1	18	2	18	1
CCL9	1322	28	1377	40	4190	120	4258	29
Ccr1	160	9	159	7	172	13	190	9
Ccr5	223	2	203	4	170	24	129	4
Ccr7	4969	165	6106	171	3623	231	7997	167
CD23	10	0	9	3	16	4	9	1
CD40	295	11	363	10	4230	149	2944	25
CD64	171	22	165	10	219	18	354	21
CD80	138	9	143	3	378	33	271	4
CD86	104	11	93	9	363	30	250	11
Cox2	25	1	33	4	674	16	307	18
Cxcl1	16	4	16	2	1174	37	442	12
Cxcl10 (IP10)	16	3	12	0	365	86	630	39
Cxcl2	28	2	22	3	1397	47	555	3
Cxcl5	5	2	6	1	98	8	20	1
Cxcr3	67	11	68	7	29	4	30	4
Cxcr4	1055	25	1106	46	429	36	587	17
Cxcr5	14	2	15	5	21	3	23	3
FcRγ -chain	1991	22	2043	13	2532	129	2780	58
FcγR IV	196	10	172	24	130	16	155	11
Hprt1	151	3	158	8	175	9	139	3
Hsp90ab1	843	2	859	5	1187	45	1403	29
human FcεR1 α	1032	24	1085	48	1350	95	2026	47
IDO1	16	5	20	2	27	3	20	1
IL-10	4	1	9	0	42	3	26	7
IL-12a (p35)	2	1	3	1	20	1	22	2
IL-12b (p40)	386	6	476	12	8518	475	926	5

Continuation* of *Table S1

	NP-OVA		NP-OVA + IgE		NP-OVA + CpG DNA		NP-OVA + papain	
mRNA* (direct counts)	**Mean**	**+/- SEM**	**Mean**	**+/- SEM**	**Mean**	**+/- SEM**	**Mean**	**+/- SEM**
IL-13	**11**	*3*	**12**	*0*	**20**	*4*	**12**	*4*
IL-15	**139**	*2*	**159**	*4*	**278**	*18*	**390**	*7*
IL-17a	**10**	*2*	**10**	*2*	**28**	*2*	**31**	*1*
IL-17E (IL-25)	**18**	*3*	**12**	*2*	**41**	*1*	**40**	*5*
IL-17F	**6**	*1*	**5**	*2*	**11**	*0*	**11**	*1*
IL-18	**67**	*3*	**63**	*7*	**98**	*8*	**95**	*6*
IL-1α	**24**	*3*	**24**	*2*	**349**	*40*	**451**	*16*
IL-1β	**306**	*8*	**365**	*33*	**2946**	*246*	**1028**	*11*
IL-23a	**17**	*4*	**19**	*1*	**27**	*4*	**25**	*4*
IL-4	**10**	*3*	**9**	*1*	**14**	*3*	**10**	*2*
IL-5	**32**	*3*	**25**	*4*	**86**	*12*	**88**	*9*
IL-6	**86**	*5*	**91**	*6*	**1521**	*74*	**544**	*8*
IL-9	**8**	*1*	**9**	*1*	**10**	*2*	**10**	*3*
IFN-β1	**6**	*2*	**9**	*1*	**15**	*2*	**8**	*2*
IFN-γ	**9**	*1*	**6**	*1*	**13**	*2*	**10**	*1*
Itgax (CD11c)	**603**	*13*	**499**	*25*	**616**	*62*	**613**	*13*
Itgb2 (CD18)	**1616**	*27*	**1650**	*82*	**1513**	*102*	**1409**	*29*
Jag1	**123**	*2*	**138**	*3*	**482**	*24*	**316**	*4*
Jag2	**10**	*1*	**11**	*2*	**10**	*2*	**7**	*1*
mouse FcεR1 α	**15**	*4*	**11**	*2*	**23**	*2*	**22**	*1*
mouse FcεR1 β	**4**	*1*	**4**	*0*	**3**	*0*	**3**	*0*
Nos2	**10**	*2*	**7**	*1*	**18**	*1*	**23**	*2*
PPAR-γ	58	*3*	**54**	*4*	**29**	*4*	**15**	*2*
PTGSE2	43	*3*	**25**	*1*	**40**	*4*	**30**	*2*
raldh1a1	6	*2*	**6**	*1*	**6**	*2*	**4**	*1*
raldh1a2	**26**	*2*	**20**	*1*	**24**	*4*	**27**	*5*
raldh1a3	**4**	*1*	**8**	*1*	**8**	*0*	**7**	*1*
Shfm1	**1216**	*4*	**1212**	*15*	**1297**	*10*	**1311**	*8*
TGF-β1	**1005**	*15*	**1057**	*37*	**1008**	*82*	**794**	*20*
Tim2	**11**	*0*	**18**	*4*	**18**	*4*	**17**	*2*
Tim3	**98**	*2*	**88**	*7*	**53**	*9*	**56**	*1*
TIM4	**29**	*6*	**30**	*1*	**60**	*4*	**43**	*1*
TNF-α	**102**	*1*	**102**	*8*	**3875**	*320*	**1398**	*28*
Tomm7	**2123**	*8*	**2132**	*27*	**1992**	*16*	**1970**	*13*
TSLP	**13**	*2*	**10**	*1*	**19**	*1*	**15**	*0*

Table S2: **mRNA expression pattern of small intestinal tissue from a representative food allergy experiment.** ([a] PBS/alum = not sensitized, [b] OVA/alum = sensitized)

	WT(-) [a]	WT(+) [b]	TG(-) [a]	TG(+) [b]
raldh1a1	119940	51028	124449	55254
Claudin 7	46545	44772	46202	43133
CCL-24 (eotaxin2)	16571	6124	11621	6801
CCL-5 (RANTES)	7847	5980	11408	5573
Mcpt1 (mast cell protease 1)	7417	1155732	4768	736576
Claudin 2	7399	12152	8239	8383
Mcpt2 (mast cell protease 2)	5155	521442	2842	324659
TGFβ-1	4721	5375	3623	6082
IL-33	4716	6856	4930	5598
FcRγ- chain	3589	5030	4035	5468
CD11c	3474	3636	3212	5267
CD103	3466	7666	3574	6968
raldh1a2	2758	2595	2582	3323
CD8 alpha	2546	1597	2783	1433
CD3 epsilon	1971	1212	1916	1188
IL-15	1582	848	1423	968
CXCL11(I-TAC)	1357	833	1373	889
IL-9	1094	463	1080	549
IL-1a	574	422	390	299
Cxcl10 (IP10)	552	387	534	417
mouse FcεRI alpha	518	36538	270	20007
CPA3 (Carboxypeptidase 3A)	454	28069	292	15022
CCL-8 (MCP-2)	409	10834	389	5598
CCL-3 (MIP-1a)	312	264	353	288
CCL-17 (TARC)	226	335	215	183
TSLP	171	266	208	256
CCR4	87	167	45	125
mouse FcεRI beta	84	6415	57	4079
IL17-F	83	60	97	63
IL12-b	73	66	66	74
IL-4	67	960	56	694
IL17E (IL-25)	59	82	81	61
IL-13	56	205	55	77
IL-6	50	553	37	342
human FcεRI alpha	47	40	10981	28620
IL-17a	45	98	27	88
CCL-7 (MCP-3)	34	157	33	109
IL-10	23	160	25	90
IFN-γ	13	108	11	106
IL-5	12	108	6	66

Figures for Reviewers

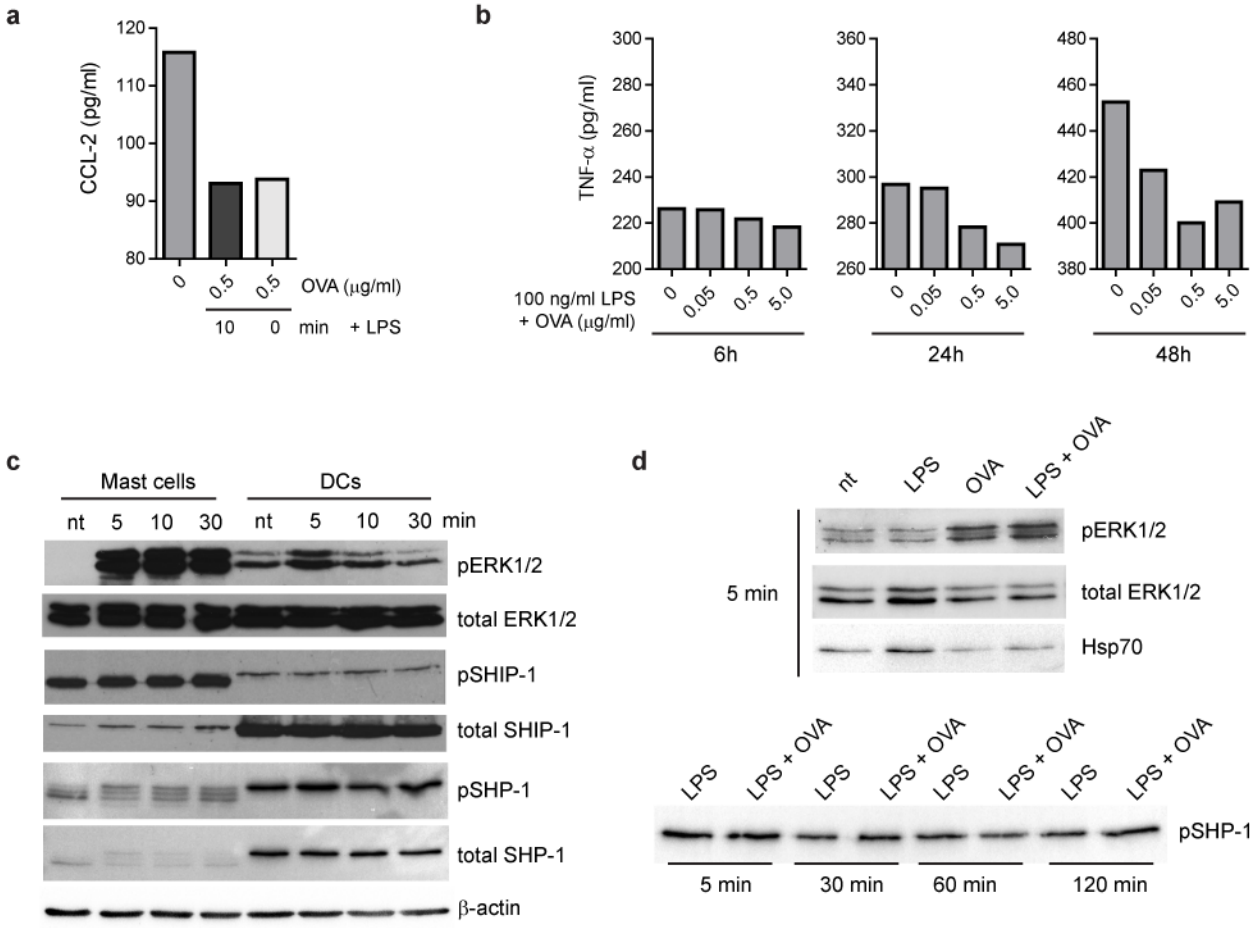

Figure R1 Additional data regarding antigen-mediated IgE/FcεRI cross-linking. **(a)** LPS-induced CCL-2 production is inhibited independently of simultaneous or consecutive FcεRI cross-linking. IgE-loaded DCs were stimulated with LPS (all conditions). Indicated concentrations of OVA were added for IgE/ FcεRI crosslinking, either simultanously with LPS (0 min) or after 10 min. Culture supernatant was harvested after 48h and CCL-2 production was analyzed by ELISA. Data are represeative of pooled triplicates. **(b)** Time course and antigen dose response experiments. DCs were stimulated with indicated concentrations of OVA and cell culture supernatants were analyzed after 6h, 24h and 48h. Inhibition of CCL2 production becomes more obviosue over the time course. **(c)** Comparison of signaling events induced upon anitgen-mediated FcεRI cross-linking in mast cells and DCs. Bone-marrow derived mast cells and DCs were pre-loaded with NP-specific IgE. Receptor crosslinking was induced with 0.5µg/ml NP-OVA, cell extracts were prepared after indicated time points, and signaling molecules were analyzed by immunoblot. **(d)** FcεRI cross-linking does not lead to increased SHP-1 phosphorylation upon LPS co-stimulation. IgE-loaded DCs were co-stimulated with LPS and NP-OVA as indicated and signaling molecules were analyzed by immunoblot.

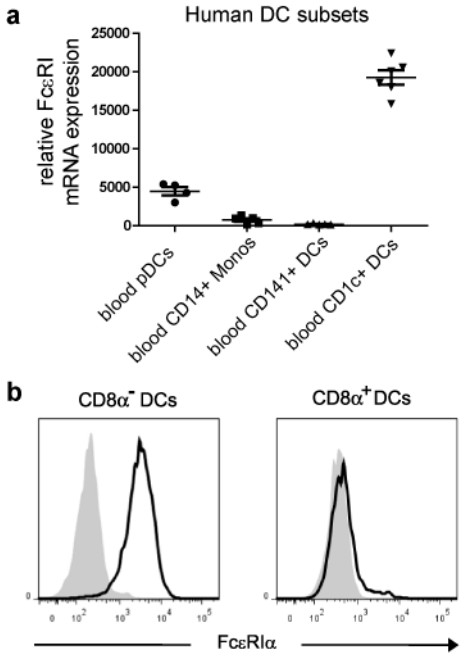

Figure R2 Comparison of FcεRI expression in human DCs subsets and DCs from IgER-TG animals. **(a)** We used publically available microarray data (Haniffa et al., 2012, Immunity 37:60-73: Human tissues contain CD141^{hi} cross-presenting dendritic cells with functional homology to mouse CD103+ nonlymphoid dendritic cells.) to define expression levels of FcεRI in different human DC populations from healthy individuals. Human CD1c^{+} DCs are defined as functional homologues of murine CD8α^{-} DCs and showed the highest transcript levels of FcεRI. FcεRI is further expressed in pDCs and, albeit at a rather low level, in CD14^{+} monocytes. No transcripts were detected in human CD141^{+} (BDCA3) DCs which are the homologues of murine CD8α^{+} DCs. **(b)** The human DC subset expression pattern of FcεRI at steady state is accurately phenocopied in splenic DCs from IgE$_R$-TG mice with high levels of surface receptor expression on CD8α^{-} DCs.